

Liquid–vapour phase behaviour of a polydisperse Lennard-Jones fluid

This article has been downloaded from IOPscience. Please scroll down to see the full text article.

2005 J. Phys.: Condens. Matter 17 S3245

(<http://iopscience.iop.org/0953-8984/17/45/008>)

View [the table of contents for this issue](#), or go to the [journal homepage](#) for more

Download details:

IP Address: 129.252.86.83

The article was downloaded on 28/05/2010 at 06:40

Please note that [terms and conditions apply](#).

Liquid–vapour phase behaviour of a polydisperse Lennard-Jones fluid

Nigel B Wilding^{1,3} and Peter Sollich²

¹ Department of Physics, University of Bath, Claverton Down, Bath BA2 7AY, UK

² King's College London, Department of Mathematics, Strand, London WC2R 2LS, UK

E-mail: N.B.Wilding@bath.ac.uk

Received 5 October 2005

Published 28 October 2005

Online at stacks.iop.org/JPhysCM/17/S3245

Abstract

We describe a simulation study of the liquid–vapour phase behaviour of a model polydisperse fluid. Particle interactions are given by a Lennard-Jones potential in which polydispersity features both in the particle sizes and the amplitude of their interactions. We address the computational problem of accurately locating the cloud curve for such a system using Monte Carlo simulations within the grand canonical ensemble. The strongly nonlinear variation of the fractional volumes of the phases across the coexistence region precludes naive extrapolation to determine the cloud point density. Instead we propose an improved estimator for the cloud point location and use scaling arguments to predict its finite-size behaviour. Excellent agreement is found with the simulation results. Application of the method reveals that the measured cloud curve is highly sensitive to the presence of large particles, even when they are extremely rare. This finding is expected to have implications for the reproducibility of experimentally measured phase diagrams in colloids and polymers.

1. Introduction

Complex fluids in which the particles are similar in character but not strictly identical are termed polydisperse. Examples arise throughout soft matter science, notably in colloidal dispersions, polymer solutions and liquid-crystals. Typically the polydispersity of such systems is manifest as variation in some physical attribute such as particle size, shape or charge, which is customarily denoted by a continuous parameter σ . The state of the system is then specified by a density distribution $\rho(\sigma)$ measuring the number density of particles of each σ [1]. The most common experimental situation is one in which the form of the overall or ‘parent’ distribution $\rho^0(\sigma)$ is fixed by the synthesis of the fluid, and only its scale can vary

³ Author to whom any correspondence should be addressed.

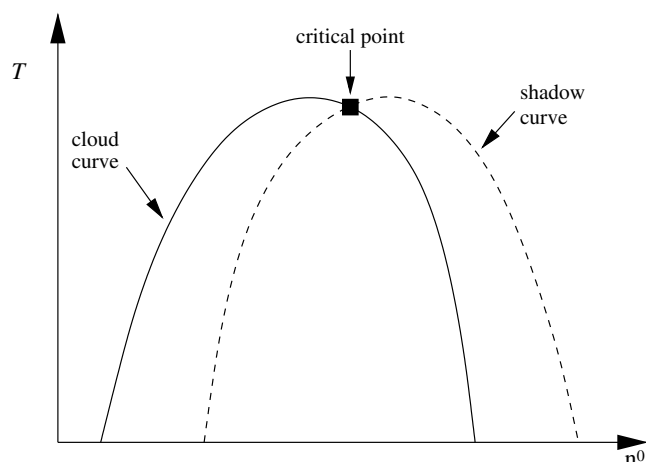


Figure 1. Schematic phase diagram of a polydisperse system in the n^0 - T plane.

depending on the proportion of the sample volume occupied by solvent. Accordingly one can write $\rho^0(\sigma) = n^0 f^0(\sigma)$, where $f^0(\sigma)$ is the normalized parent shape function and $n^0 = N/V$ the overall particle number density. Varying n^0 at a given temperature corresponds to scanning a ‘dilution line’ of the system.

Polydisperse fluids differ from their monodisperse counterparts in a variety of aspects. Principal among these is the far richer character of their phase behaviour [2]. This richness is traceable to *fractionation* effects. At phase coexistence, particles of each σ may partition themselves *unevenly* between two (or more) coexisting ‘daughter’ phases as long as—due to particle conservation—the overall composition $\rho^0(\sigma)$ of the parent phase is maintained. This partitioning can have dramatic consequences for phase diagrams. For example, the conventional liquid–gas binodal of a monodisperse system (which connects the ends of tie-lines in a density–temperature diagram) splits into a ‘cloud’ and a ‘shadow’ curve, as shown schematically in figure 1. These give, respectively, the density at which phase coexistence first occurs and the density of the incipient phase; the curves do not coincide because the shadow phase in general differs in composition from the parent. Furthermore, as observed in many experiments (see e.g. [3]) the critical point lies not at the maximum of the cloud or shadow curve, but at their intersection.

Only recently has experimental work started to elucidate (in a systematic fashion) the generic consequences of fractionation for phase coexistence properties [4, 5] and many unsolved issues remain. In this paper, we employ simulation within the grand canonical ensemble (GCE) to investigate the phase behaviour of a model polydisperse fluid in which particles interact via a Lennard-Jones potential. The form of the interactions is such that polydispersity affects both the particles’ diameters σ and the amplitude of interactions. Such a model yields a phase diagram of the form figure 1⁴. Our results show that fractionation effects severely complicate the task of accurately determining cloud points for the system. To address this problem we propose an improved estimator for the location of the cloud point, and analyse its finite-size scaling properties. The simulation results are found to be in good agreement with the theoretical predictions.

⁴ In previous work, we showed that if polydispersity of particles sizes, but not amplitudes, is considered, then the critical point instead lies very close to the maximum of the cloud curve [13].

2. Model and computational methods

Our model comprises a fluid of particles interacting via a Lennard-Jones potential:

$$u_{ij} = \epsilon_{ij} \left[(\sigma_{ij}/r_{ij})^{12} - (\sigma_{ij}/r_{ij})^6 \right], \quad (1)$$

with $\epsilon_{ij} = \sigma_i \sigma_j$, $\sigma_{ij} = (\sigma_i + \sigma_j)/2$ and $r_{ij} = |\mathbf{r}_i - \mathbf{r}_j|$. Although this choice of mixing rules is non-standard in terms of those commonly employed for simple binary mixtures, it has the advantage in the present context of considerably simplifying theoretical phase behaviour calculations made using the moment free energy method, details of which we report elsewhere [6]. We do not expect the qualitative features of our results to be sensitive to whether one uses the above mixing rules, or more standard ones such as Lorentz–Bertholet rules [7].

The potential was truncated for $r_{ij} > 2.5\sigma_{ij}$ and no tail corrections were applied. The diameters σ are drawn from a (parental) Schulz distribution $f^0(\sigma) \propto \sigma^z \exp[(z+1)\sigma/\bar{\sigma}]$, with a mean diameter $\bar{\sigma}$ which sets our unit length scale. We elect to study the case $z = 50$, corresponding to a moderate degree of polydispersity: the standard deviation of particle sizes is $\delta \equiv 1/\sqrt{z+1} \approx 14\%$ of the mean. The distribution $f^0(\sigma)$ was truncated to within the range $0.5 < \sigma < \sigma_c$. The upper cutoff σ_c serves to prevent the appearance of arbitrarily large particles in the simulation, but would also be expected in experimental systems because in the chemical synthesis of colloid particles, time or solute limits restrict the maximum particle size [8].

The GCE is the ensemble of choice for simulations of polydisperse fluids because it permits sampling of many different realizations of the instantaneous particle size distribution, while catering naturally for fractionation effects at phase coexistence. Operationally, we ensure that the ensemble-averaged density distribution always equals the desired parent distribution $\rho^0(\sigma)$ by controlling an imposed chemical potential distribution $\mu(\sigma)$. This is achieved using the non-equilibrium potential refinement (NEPR) scheme [9], which enables the efficient iterative determination of $\mu[\rho^0(\sigma), T]$, from a single simulation run, and without the need for an initial guess of its form. To achieve this, the method continually updates $\mu(\sigma)$ in such a way as to minimize the deviation of the instantaneous density distribution $\rho(\sigma)$ from the target form (i.e. the parent). However, tuning $\mu(\sigma)$ in this manner clearly violates detailed balance. To correct this, successive iterations reduce the degree of modification applied to $\mu(\sigma)$, thereby driving the system towards equilibrium and ultimately yielding the equilibrium form of $\mu[\rho^0(\sigma), T]$. Once the requisite form of $\mu(\sigma)$ has been determined for one point on the dilution line, histogram reweighting permits extrapolation to nearby points [10].

3. Results and finite-size scaling analysis

The principal observable in the GCE simulations is the probability distribution of the fluctuating number density $p(n)$. We have obtained the form of $p(n)$ for a range of parent densities n^0 at $T = T_c$. Note that here we merely use T_c as a convenient reference point; for our system, coexistence occurs at T_c over a range of parent densities n^0 (cf figure 1), in contrast to the monodisperse case. Figure 2 shows that in the coexistence region $p(n)$ has two distinct peaks, which we sample using multicanonical preweighting [11]. The weight under the low and high density peaks corresponds respectively to the fractional volumes v_g and v_l that would be occupied by gas and liquid in the corresponding canonical ensemble. As expected, the peaks separate and the valley between them deepens as we move away from the critical point by decreasing n^0 . This is accompanied by a gradual transfer of weight from the liquid to the gas peak. Finally the liquid peak disappears, at exponentially small values of v_l visible only on a log scale (figure 2(b)).

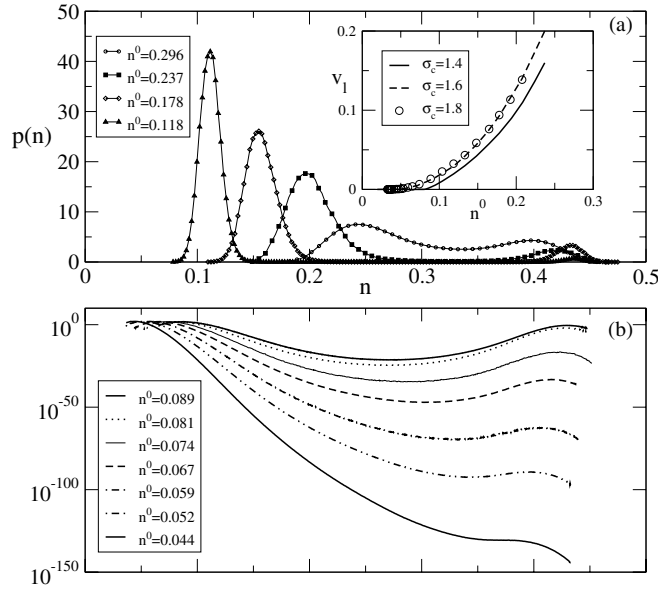


Figure 2. Number density distribution $p(n)$ at $T = T_c$ for parent densities n^0 as indicated and for particle size cutoff $\sigma_c = 1.4$. (a) Linear and (b) log scale. Inset: liquid fractional volume v_l versus n^0 , for $\sigma_c = 1.4, 1.6, 1.8$.

The observed variation of $p(n)$ poses the question of how to detect the cloud point n_{cl}^0 , defined as the lowest parent density n^0 where stable phase coexistence occurs. This is simple in a monodisperse system because the cloud point also gives the density of the gas phase, which remains constant throughout the coexistence region. One then simply detects the point where the gas and liquid peaks have the same weight, i.e. $r = v_l/v_g = 1$, and measures the gas density there. (The criterion $r = 1$ has the added advantage of leading to only exponentially small finite-size corrections to the value of μ at coexistence [12].) However, in a polydisperse system this method fails because fractionation causes the densities and size distributions of the coexisting phases to vary with n^0 [2]. One could attempt to locate the cloud point instead by extrapolating in n^0 to the point where $v_l \rightarrow 0$ [13]. But in our system the dependence of v_l on n^0 is so strongly nonlinear—another effect of fractionation, see the inset of figure 2—that the resulting cloud point estimates would have very large error bars. Indeed, on a linear plot of v_l versus n^0 , as shown in figure 2(a), the particle size cutoff effects which our more careful analysis will reveal (see figure 4 below) would be essentially invisible.

In order to address this problem we analyse the finite-size scaling of $p(n)$. As the linear system size L grows at fixed n^0 and T , the peaks in $p(n)$ will narrow around the densities of gas and liquid, respectively, and the size distributions averaged over configurations from each peak will tend to those in the coexisting phases. The ratio $r = v_l/v_g$ is determined by the difference in the grand potential. The latter is directly related to the pressure P difference between the phases i.e. $r = \exp(\beta L^d \Delta P)$ for large L , where $\beta = 1/k_B T$ and $\Delta P = P_l - P_g$. The criterion for stable coexistence at given fixed n^0 is that r must have a finite value as $L \rightarrow \infty$; the pressure difference then has to scale as $\Delta P \sim L^{-d}$ except in the special case $r = 1$ (see above).

For finite L , the liquid phase coexists metastably with the gas in the density region $n^0 < n_{cl}^0$, where $\Delta P = O(1)$, but here r will be exponentially small. Figure 3 shows this effect clearly:

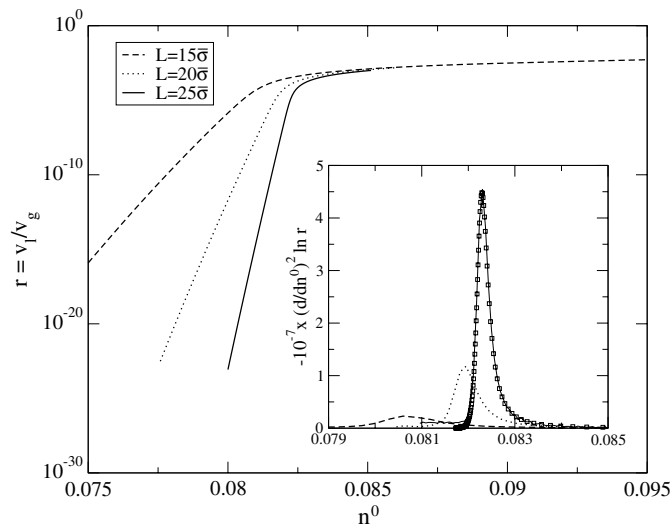


Figure 3. Ratio r of liquid to gas fractional volumes on approach to the cloud point at $T = T_c$ for $\sigma_c = 1.4$. The inset shows the second derivative of $\ln r$ w.r.t. n^0 . The peak position gives an estimate of the cloud point density. Squares indicate the scaled universal master curve (equation (2)).

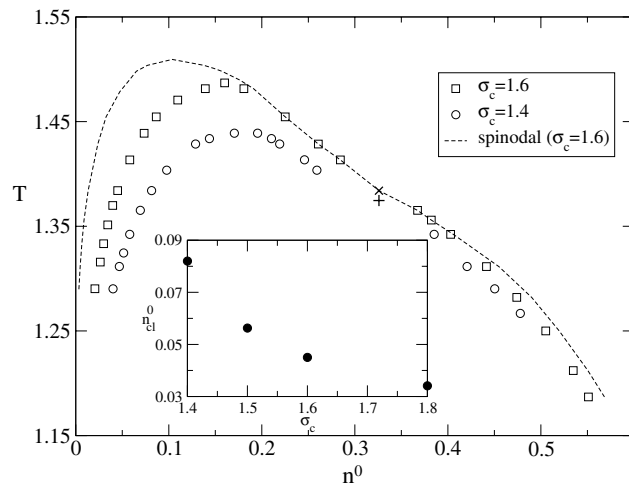


Figure 4. Comparison of cloud curves for $\sigma_c = 1.4$ and 1.6 . The critical points for $\sigma_c = 1.6$ (\times) and $\sigma_c = 1.4$ ($+$) are marked. Also shown is the effect spinodal (limit of metastability) for $\sigma_c = 1.6$ for $L = 15\bar{\sigma}$. The inset displays the variation of the gas cloud point density n_{cl}^0 at $T = T_c$ as a function of σ_c .

r is independent of L for large enough n^0 , but the curves separate strongly (note the log scale) for smaller n^0 . The cloud point separates the two regimes, permitting the estimate $n_{cl}^0 \approx 0.0825 \pm 0.0005$ for the parameters shown in the figure.

One can estimate n_{cl}^0 even from data for only a single system size L , by using the fact that ΔP is $O(1)$ and scales linearly with $n^0 - n_{cl}^0$ to leading order near the cloud point, which implies $\ln r \sim L^d(n^0 - n_{cl}^0)$. This applies for $n^0 < n_{cl}^0$, while above n_{cl}^0 one has $\ln r = O(1)$. Thus the derivative $(\partial/\partial n^0) \ln r$ should drop from an $O(L^d)$ plateau to $O(1)$ around $n^0 = n_{cl}^0$.

In the second derivative $-(\partial/\partial n^0)^2 \ln r$ this drop will manifest itself as a peak. A smooth derivative can be extracted from simulation data using histogram reweighting, and the peak position then serves as an estimate for n_{cl}^0 . This is shown in the inset of figure 3, and gives $n_{\text{cl}}^0 \approx 0.0823$ from the largest L , consistent with our earlier estimate derived from comparing data for different L .

The above arguments can be formalized using the results of [12], which pertain to the monodisperse case but which we have generalized to polydisperse systems [14]. We find that for large L the second-derivative plot approaches a master curve

$$-\left(\frac{\partial}{\partial \tilde{n}^0}\right)^2 \ln r = \frac{z}{(1+z)^3}, \quad \tilde{n}^0 = z + \ln z, \quad (2)$$

parameterized by z . The scaled parent density is defined here as $\tilde{n}^0 = aL^d(n^0 - n_{\text{cl}}^0) + \ln(bL^d n_{\text{cl}}^0)$ with a and b system-dependent dimensionless scaling factors. This scaling implies that the cloud point estimate from the peak position has finite-size corrections of order $L^{-d} \ln L$, while the peak width and height scale as L^{-d} and L^{2d} , respectively. Our data are consistent with the width and height scaling and with the dominant L^{-d} dependence of the peak shifts [14]. The master curve (equation (2)), appropriately scaled, is overlaid onto the largest- L data in figure 3 (inset) and shows excellent agreement.

One observes from figure 2 that the metastable liquid peak in $p(n)$ persists until well below the cloud point n_{cl}^0 . The value of n^0 at which it disappears marks the so-called effective spinodal point [15] at which the liquid is no longer stable to small density fluctuations. The parent density n_{sp}^0 where this occurs should tend to the cloud curve as L grows large [15]. Spinodals in monodisperse systems are conventionally characterized by the density of the phase that becomes unstable, which is located inside the region where phase separation occurs. Here we use instead the density n_{sp}^0 of the coexisting *stable* phase, which is outside this region. This is a more meaningful representation in the polydisperse context since only the stable (majority) phase has the parental size distribution, while that of the metastable (minority) phase is determined indirectly via chemical potential equality.

With regard to the overall phase diagram of our system, the cloud curve as calculated using the methods describe above is presented in figure 4 for two choices of the upper cutoff on the density distribution, $\sigma_c = 1.4$ and 1.6. One observes a strong dependence of these curves on the cutoff, even though both values of σ_c are far in the tail of the parent distribution. This arises from very strong fractionation effects (figure 5): even though particle sizes around σ_c are very rare in the parent, they occur in significant concentration in the shadow liquid. Physically, the large particles interact more strongly and therefore lead to a significant gain in free energy at the shorter interparticle separations in the liquid.

It is natural to ask whether the gas phase cloud point density would tend to a non-zero limit as σ_c is increased. Indeed the inset of figure 4 shows a further strong decrease of n_{cl}^0 by $\approx 25\%$ between $\sigma_c = 1.6$ and 1.8. Theoretical predictions of a moment free energy calculation for a van der Waals model free energy [13, 14] suggest that this trend continues and that the cloud point density approaches zero for large σ_c . Such an unusual effect has previously been seen in polydisperse hard rods with wide length distributions [16], though only for large σ_c and distributions with fatter than exponential tails. Here the decrease of n_{cl}^0 is clear even for σ_c of the same order as $\bar{\sigma}$, and scaling estimates suggest that cutoff effects occur for any size distribution with tails heavier than a Gaussian [14].

The physical origin of the decrease of n_{cl}^0 to zero is that for large σ_c the size distribution in the shadow liquid develops a second peak near $\sigma \approx \sigma_c$ [14]. We expect this to become dominant eventually so that as σ_c increases the shadow will consist of ever more strongly interacting particles whose sizes are concentrated near the cutoff. It seems reasonable to

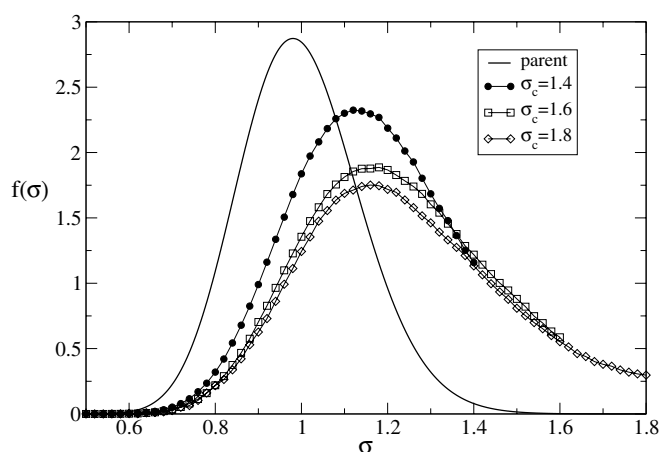


Figure 5. Size distributions $f(\sigma)$ in the liquid shadow phase distributions at $T = T_c$ for $\sigma_c = 1.4, 1.6, 1.8$. Also shown is the parent distribution $f^0(\sigma)$.

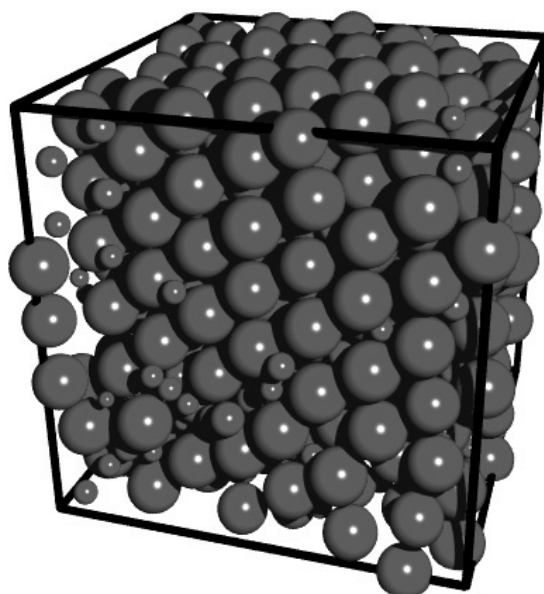


Figure 6. A snapshot of the quasi-monodisperse crystalline phase that forms from the metastable liquid near the spinodal for $\sigma_c = 2.8, T = T_c$; see text for details.

postulate that, as a consequence, there should exist some cutoff for which the shadow phase liquid freezes into a quasi-monodisperse crystal phase. Indeed our simulations provide some evidence for just such a scenario. Specifically, for the large cutoff value $\sigma_c = 2.8$ and for small n^0 values lying near the spinodal, we observe spontaneous freezing of the metastable liquid to an fcc crystal structure (see figure 6) [14]. This finding suggests that it is indeed possible that, for cutoff values larger than those presently accessible in our simulations, the freezing might occur from a stable liquid phase shadow. Even in the metastable case, however, it could be possible to observe the crystalline phase in a ‘wetting’ experiment where an attractive wall stabilizes a finite volume of the dense phase.

Finally we note from the cloud curves (figure 4) that significant cutoff-dependent shifts occur only for densities below the critical density. This is consistent with our interpretation above: for higher densities, the shadow phase is a gas phase of *lower* density than the parent. In this, the concentration of large particles is *suppressed* and that of small particles negligibly enhanced because of their weak interactions. The shadow size distributions are therefore concentrated well within the range $0.5 \dots \sigma_c$ (data not shown) so that no cutoff dependence arises.

4. Conclusions

To summarize, fractionation effects pose distinct problems for simulation studies of the phase behaviour of polydisperse fluids. We have presented a generally applicable finite-size scaling method which addresses this matter. Application to a model system reveals that the locus of the cloud curve is highly sensitive to the imposed value of the particle size cutoff: large particles have an influence on the phase behaviour which is disproportionate to their overall concentration. Such effects imply that in experiments on polydisperse fluids (see e.g. [5]) it may be important to monitor and control carefully the tails of the size (or charge, etc) distribution. Otherwise undetected differences could lead to irreproducibility in the observed phase behaviour of ostensibly identical samples.

References

- [1] Salacuse J J and Stell G 1982 *J. Chem. Phys.* **77** 3714
- [2] Sollich P 2002 *J. Phys.: Condens. Matter* **14** R79
- [3] Kita R, Kubota K and Dobashi T 1997 *Phys. Rev. E* **56** 3213
- [4] Evans R M L, Fairhurst D J and Poon W C K 1998 *Phys. Rev. Lett.* **81** 1326
- [5] Ern e B H, Van den Pol E, Vroege G J, Visser T and Wensink H H 2005 *Langmuir* **21** 1802
- [6] Wilding N B, Sollich P and Fasolo M 2005 *Phys. Rev. Lett.* **95** 155701
- [7] Allen M P and Tildesley D J 1989 *Computer Simulation of Liquids* (Oxford: University Press)
- [8] Kvitek L, Pucek R, Pan a ek A, Novotn y R, Hrb a c J and Zbořil R 2005 *J. Mater. Chem.* **15** 1099
- [9] Wilding N B 2003 *J. Chem. Phys.* **119** 12163
Wilding N B and Sollich P 2002 *J. Chem. Phys.* **116** 7116
- [10] Ferrenberg A M and Swendsen R H 1988 *Phys. Rev. Lett.* **61** 2635
Ferrenberg A M and Swendsen R H 1989 *Phys. Rev. Lett.* **63** 1195
- [11] Berg B A and Neuhaus T 1992 *Phys. Rev. Lett.* **68** 9
- [12] Borgs C and Janke W 1992 *Phys. Rev. Lett.* **68** 1738
Borgs C and Kotecky R 1992 *Phys. Rev. Lett.* **68** 1734
- [13] Wilding N B, Fasolo M and Sollich P 2004 *J. Chem. Phys.* **121** 6887
- [14] Wilding N B, Fasolo M and Sollich P, unpublished
- [15] Binder K 2003 *Physica A* **319** 99
- [16] Speranza A and Sollich P 2003 *J. Chem. Phys.* **118** 5213